Published in final edited form as:

Neuron. 2014 October 01; 84(1): 123–136. doi:10.1016/j.neuron.2014.08.056.

GINIP, a $G_{\alpha i}$-Interacting Protein, Functions as a Key Modulator of Peripheral $GABA_B$ Receptor-Mediated Analgesia

Stéphane Gaillard[1,10], **Laure Lo Re**[1,10], **Annabelle Mantilleri**[1], **Régine Hepp**[2,3,4], **Louise Urien**[1], **Pascale Malapert**[1], **Serge Alonso**[1], **Michael Deage**[5], **Charline Kambrun**[6,7], **Marc Landry**[6,7], **Sarah A. Low**[8], **Abdelkrim Alloui**[9], **Bertrand Lambolez**[2,3,4], **Grégory Scherrer**[8], **Yves Le Feuvre**[6,7], **Emmanuel Bourinet**[5], **Aziz Moqrich**[1,*]

[1]Aix-Marseille-Université, CNRS, Institut de Biologie du Développement de Marseille, UMR 7288, case 907, 13288 Marseille Cedex 09, France

[2]Sorbonne Universités, UPMC Univ Paris 06, UM CR 18, Neuroscience Paris Seine, 75005 Paris, France

[3]Centre National de la Recherche Scientifique (CNRS), UMR 8246 Paris, France

[4]Institut national de la Santé et de la Recherche Médicale (INSERM), UMR-S 1130 Paris, France

[5]Laboratories of Excellence, Ion Channel Science and Therapeutics, Institut de Génomique Fonctionnelle, UMR 5203, CNRS, U661, INSERM, Universités Montpellier I&II, 141 Rue de la Cardonille, 34094 Montpellier Cedex 05, France

[6]University Bordeaux, Interdisciplinary Institute for Neuroscience, UMR 5297, 33000 Bordeaux, France

[7]CNRS, Interdisciplinary Institute for Neuroscience, UMR 5297, 33000 Bordeaux, France

[8]Department of Anesthesiology, Perioperative and Pain Medicine, Department of Molecular and Cellular Physiology, Stanford Neurosciences Institute, Stanford University, Palo Alto, CA 94304, USA

[9]Laboratoire de Pharmacologie Médicale, Faculté de Médecine et de Pharmacie, UMR 766 INSERM, 28 place Henri-Dunant, BP 38, 63001 Clermont-Ferrand Cedex 1, France

[10]Co-first author

SUMMARY

One feature of neuropathic pain is a reduced GABAergic inhibitory function. Nociceptors have been suggested to play a key role in this process. However, the mechanisms behind nociceptor-

*Correspondence: aziz.moqrich@univ-amu.fr.

AUTHOR CONTRIBUTIONS

A. Moqrich designed the project and S.G. generated the knockin mouse model. S.G., L.L.R., A. Mantilleri, and L.U. performed functional characterization of GINIP mice. S.A. performed Southern blot screening, M.D. and E.B. performed BRET and electrophysiological experiments on DRG neurons, C.K., M.L., and Y.L.F. performed spinal cord electrophysiological recordings, R.H. and B.L. performed the FRET experiments on DRG neurons, A.A. performed the CCI experiments, G.S. and S.A.L. performed the GINIP/MOR and GINIP/DOR coexpression analysis, and P.M. provided logistical help. A.Moqrich wrote the paper.

SUPPLEMENTAL INFORMATION

Supplemental Information includes Supplemental Experimental Procedures and four figures and can be found with this article online at http://dx.doi.org/10.1016/j.neuron.2014.08.056.

mediated modulation of GABA signaling remain to be elucidated. Here we describe the identification of GINIP, a $G_{\alpha i}$-interacting protein expressed in two distinct subsets of nonpeptidergic nociceptors. GINIP null mice develop a selective and prolonged mechanical hypersensitivity in models of inflammation and neuropathy. GINIP null mice show impaired responsiveness to $GABA_B$, but not to delta or mu opioid receptor agonist-mediated analgesia specifically in the spared nerve injury (SNI) model. Consistently, GINIP-deficient dorsal root ganglia neurons had lower baclofen-evoked inhibition of high-voltage-activated calcium channels and a defective presynaptic inhibition of lamina IIi interneurons. These results further support the role of unmyelinated C fibers in injury-induced modulation of spinal GABAergic inhibition and identify GINIP as a key modulator of peripherally evoked $GABA_B$-receptors signaling.

INTRODUCTION

Peripheral nerve injury leading to chronic pain is one of the most challenging types of pain to manage. Chronic pain is associated with a marked imbalance between excitatory and inhibitory neurotransmission in the dorsal horn of the spinal cord, leading to a state of persistent pain. In these conditions, pain arises spontaneously, noxious stimuli evoke an exaggerated and prolonged response (hyperalgesia), and innocuous stimuli become painful (allodynia) (Latremoliere and Woolf, 2009). Recent studies using a combination of genetic and pharmacological neuronal ablation have shown that nociceptive neurons play a pivotal role in pain sensation in a modality-specific manner (Abrahamsen et al., 2008; Cavanaugh et al., 2009; Han et al., 2013; Li et al., 2011; Scherrer et al., 2009; Shields et al., 2010; Vrontou et al., 2013). Nociceptive neurons represent a major site of action for pain killer therapies, as most analgesic drugs (i.e., opioids, cannabinoids, and GABA derivatives) are known to influence nociceptive terminals (Agarwal et al., 2007; Janson and Stein, 2003; Scherrer et al., 2009; Takeda et al., 2004). Together, these arguments suggest that an efficient treatment of pain requires an extensive understanding of nociceptive neuronal physiology as well as the mechanisms that operate under pathological conditions to perpetuate pain perception. Furthermore, targeting painkiller drugs to primary nociceptive neurons might be particularly advantageous as they would bypass side effects related to central activity.

The heterotrimeric G protein-coupled receptors (GPCRs) represent the largest and most diverse family of cell surface receptors. Their cellular localization and mode of action make them the most targeted receptors for pain therapy. Among these, $GABA_B$ receptors ($GABA_B$-Rs) are of particular interest. $GABA_B$-Rs are found at both excitatory and inhibitory synapses in the brain (Remondes and Schuman, 2003) as well as in the superficial dorsal horn, predominantly on afferent terminals of sensory neurons (Castro et al., 2004; Charles et al., 2001; Engle et al., 2012; Gangadharan et al., 2009; Jasmin et al., 2003; Price et al., 1987; Towers et al., 2000; Yang et al., 2001). Multiple lines of evidence support an analgesic role for $GABA_B$-Rs in animal models of acute and chronic pain. Mutant mice lacking $GABA_B$ receptors exhibit exaggerated responses to acute thermal and mechanical stimuli (Gassmann et al., 2004; Schuler et al., 2001). Baclofen, a selective agonist of $GABA_B$-Rs, produces efficient analgesia in different settings of nerve injury (Hwang and Yaksh, 1997; Patel et al., 2001; Smith et al., 1994) and significantly suppresses the first and second phases of formalin-evoked pain (Dirig and Yaksh, 1995; Patel et al., 2001) but has no

effect on Complete Freund's adjuvant (CFA)-induced mechanical hyperalgesia (Hwang and Yaksh, 1997; Smith et al., 1994). Peripheral baclofen-mediated analgesia is caused by a strong inhibition of L-glutamate release from primary afferent terminals, namely the C-unmyelinated fibers (Ataka et al., 2000; Iyadomi et al., 2000) and a significant reduction of GABA and glycine release in the spinal dorsal horn (Iyadomi et al., 2000; Wang et al., 2007). Moreover, several studies have demonstrated an impairment of GABAergic inhibition in the dorsal horn of the spinal cord in several nerve injury models, such as chronic constriction injury of the sciatic nerve (CCI) and spared nerve injury (SNI) (Engle et al., 2012; Ibuki et al., 1997; Laffray et al., 2012; Moore et al., 2002), suggesting that spinal GABAergic inhibition is abnormal in neuropathic pain states. Whether primary sensory neurons are involved in this impairment of GABAergic signaling in pathological conditions remains under intense investigation.

Here we describe the identification of GINIP, a plant homeodomain (PHD) and EF-hand containing protein that preferentially interacts with Gα inhibitory proteins. GINIP is expressed in two distinct subsets of nonpeptidergic nociceptors: the cutaneous free nerve ending MRGPRD-expressing neurons and TAFA4-expressing C-low threshold mechanoreceptors (C-LTMRs) (Delfini et al., 2013; Li et al., 2011; Seal et al., 2009; Zylka et al., 2005). GINIP null mice exhibit prolonged mechanical hypersensitivity in models of inflammation and neuropathy without affecting thermal hyperalgesia. Importantly, GINIP null mice selectively resist reversal of SNI-evoked mechanical hyperalgesia by baclofen, but not by delta or mu opioid receptor agonists. Consistently, GINIP-deficient dorsal root ganglia (DRG) neurons display significantly lower baclofen-evoked inhibition of high-voltage-activated calcium channels that resulted in a defective baclofen-induced presynaptic inhibition of lamina IIi spinal cord interneurons.

RESULTS

Identification of GINIP, a $G_{\alpha i}$-Interacting Protein

In an attempt to increase the repertoire of markers defining discrete subsets of primary nociceptive neurons, we used Affimetrix microarrays to compare global gene expression profiles of DRG of wild-type and $trkA^{trkC/trkC}$ knockin mice at birth (Moqrich et al.,2004; Legha et al., 2010). Among the several hundred potential markers identified, *mkiaa1045* named *GINIP* (for *G*α *in*hibitory *i*nteracting *p*rotein) encodes a highly conserved vertebrate 400 amino acid protein of unknown function (Figure 1A). SMART program analysis showed that GINIP is endowed with two functional domains: a plant homeodomain (PHD) zinc finger and two putative EF hand domains. In order to assign a potential function to GINIP, we launched a yeast two-hybrid assay using the full-length GINIP as bait to screen an adult mouse brain cDNA library. Out of 134 million interactions tested, we identified 83 potential protein-protein interactions. Out of the 83 interactions, 44 contained $G_{\alpha i}1$ encoded by 11 independent clones, 38 contained $G_{\alpha i}3$ encoded by 6 independent clones, and 1 clone encoded a non-ATPase subunit of the proteasome Psmd11. As our yeast two-hybrid screen used a mouse brain cDNA library, we first checked the expression pattern of the three $G_{\alpha i}$ genes (*gnai1*, *gnai2*, and *gnai3*) in DRG neurons. In situ hybridization with a probe specific to endogenous *gnai1*, *gnai2*, and *gnai3*, followed by immunofluorescent labeling with a

newly generated rat anti-GINIP antibody, demonstrated that $G_{\alpha i}1$ is predominantly expressed in large-diameter neurons and largely excluded from $GINIP^+$ neurons (12.8% ± 0.16% of $GINIP^+$ neurons express $G_{\alpha i}1$, and 14.5% ± 0.18% of $G_{\alpha i}1^+$ neurons express GINIP), whereas $G_{\alpha i}2$ and $G_{\alpha i}3$ were mainly expressed in smaller-diameter neurons and showed a significant overlap with $GINIP^+$ neurons (55.1% ± 0.17% and 44% ± 0.15% of $GINIP^+$ neurons express $G_{\alpha i}2$ and $G_{\alpha i}3$, respectively, and 48.5% ± 0.11% of $G_{\alpha i}2^+$ and 54% ± 0.15% of $G_{\alpha i}3^+$ neurons express GINIP) (Figure 1B).

To validate interactions of GINIP with the three known $G_{\alpha i}$ proteins, a glutathione S-transferase (GST) pull-down assay was performed using GST-GINIP and human embryonic kidney 293T (HEK293T) cell extracts. The three $G_{\alpha i}$ proteins were fused to Venus protein and expressed in HEK293T cells as wild-type, a constitutively inactive GDP-bound mutant (G203A), or a constitutively active GTP-bound mutant (Q204L). Western blot using anti-GFP antibody to detect Venus-tagged proteins showed that GINIP interacts only with the constitutively active form of all $G_{\alpha i}$ proteins, but not with their respective wild-type or GDP-bound forms (Figure 1C and data not shown). Very interestingly, there was no interaction between GINIP and s, q, or o types of Gα subunits, indicating that GINIP exclusively participates in downstream signaling triggered by activation of $G_{\alpha i}$ proteins.

GINIP Defines Two Distinct Subsets of Nonpeptidergic Primary Sensory Neurons

To characterize the population of neurons expressing GINIP, we performed double fluorescent labeling experiments, using rat anti-GINIP antibody (see Figure 2A for specificity) in combination with a variety of subtype-specific markers of adult DRG neurons. GINIP is excluded from $TrkA^+$, $TrkB^+$, and $TrkC^+$ neurons and labels a subset of small-diameter Ret^+ neurons, namely those expressing GFRα2 (Figure 2A). Further molecular characterization showed that $GINIP^+$ neurons can be split into $GINIP^+/IB4^+$ neurons (72.3% ± 0.8%, n = 3) and $GINIP^+/IB4^-$ neurons (27.7% ± 0.4%, n = 3) (Figure 2A). Interestingly, $GINIP^+/IB4^+$ neurons express *mrgprD*, whereas $GINIP^+/IB4^-$ neurons express *TH* and *tafa4*, two previously identified markers of C-LTMRs (Figure 2A and data not shown) (Delfini et al., 2013; Li et al., 2011). GINIP was excluded from $TRPV1^+$, *trpm8*$^+$, *mrgprA1*$^+$, and *mrgprB4*$^+$ neurons, as well as from the subpopulation of neurons expressing high levels of *trpa1*, and showed a partial overlap with *mrgprA3*$^+$ neurons (Figure S1, available online). In line with its expression profile, GINIP-expressing afferents selectively target lamina II ($PKC\gamma^+$ and $IB4^+$), but not lamina I ($CGRP^+$), layers of the dorsal horn spinal cord (Figures 2B and 2C). Importantly, GINIP is not expressed in spinal cord neurons (Figures 2B and 2C). Together, our expression data show that GINIP defines two distinct subpopulations of nonpeptidergic neurons: the cutaneous free nerve ending MRGPRD-expressing neurons and C-LTMRs.

GINIP Is Dispensable for Developmental Specification of GINIP-Expressing Neurons

To gain insights into the role of GINIP in the development, maturation, and function of $GINIP^+$ neurons, we generated a knockin mouse model where the *ginip* locus has been manipulated to trigger *ginip* gene inactivation and enables genetic marking and tissue-specific neuronal ablation of GINIP-expressing neurons (Figure S2A). In this study, we focus on the GINIP loss-of-function phenotype. $GINIP^{flx/+}$ mice were crossed with mice

driving CRE recombinase in a ubiquitous manner (Schwenk et al., 1995) to produce GINIP $^{+/mcherry}$ mice. GINIP$^{+/mcherry}$ mice were then intercrossed to generate GINIP$^{mcherry/mcherry}$ and wild-type littermates (hereafter GINIP$^{-/-}$ and WT mice, respectively). GINIP$^{-/-}$ mice were viable and fertile, born in a Mendelian ratio, and indistinguishable from their control littermates. Immunolabeling using anti-GINIP antibody showed that GINIP protein was completely eliminated in GINIP$^{-/-}$ mice (Figure S2B). Thorough quantitative and qualitative analysis of different DRG neuronal subpopulations in adult GINIP$^{-/-}$ mice revealed no difference between WT and GINIP$^{-/-}$ mice. Using SCG10 as a pan-neuronal marker, we showed that DRG neuronal counts of GINIP$^{-/-}$ and WT mice were similar (Figure S2C). Consistently, quantification of TrkA^{+}, TrkB^{+}, TrkC^{+}, and Ret^{+} neurons showed no difference between GINIP$^{-/-}$ and WT DRG, and the total number of *mrgprD*$^{+}$, IB4^{+}, and *gfra2*$^{+}$ neurons in L5 neurons was indistinguishable between GINIP$^{-/-}$ and WT mice (Figure S2C). Together, these results suggest that GINIP is dispensable for the developmental specification of DRG neurons, including the neuronal class expressing this PHD and EF-hand containing protein.

GINIP Null Mice Exhibit Selective and Prolonged Injury-Induced Mechanical Hypersensitivity

To gain insights into the functional role of GINIP in GINIP^{+} neurons, we subjected GINIP $^{-/-}$ mice to a large battery of somatosensory tests under acute and tissue or nerve injury conditions. GINIP$^{-/-}$ mice appeared normal in body weight, open-field, and rotarod profiles, demonstrating that GINIP$^{-/-}$ mice do not have abnormalities in motor activity or anxiety (Figures S3A and S3B and data not shown). We then subjected GINIP$^{-/-}$ mice to a variety of thermal tests, including the thermotaxis gradient assay, hot and cold plate, and Hargreaves tests. In all these paradigms, we found no behavioral difference between GINIP$^{-/-}$ mice and their WT littermates (Figures S3C–S3F), suggesting that GINIP is dispensable for acute and injury-induced temperature sensation. To test the ability of GINIP$^{-/-}$ mice to sense chemical pain, we used the formalin test. Intraplantar injection of 10 μl of 2% formalin triggered a robust first pain response in both genotypes, but the appearance of the second pain response occurred much earlier in GINIP$^{-/-}$ compared to control littermates. However, when the total time spent in flinching, biting, and licking behavior was scored, we found no significant difference between the two genotypes during the first and the second phase (Figure 3A). We then tested GINIP$^{-/-}$ mice for their ability to sense mechanical stimuli under inflammatory and neuropathic pain conditions. In both paradigms, acute mechanical sensation was unaffected in GINIP$^{-/-}$ mice (Figures 3B and 3C). In the Carrageenan model, both genotypes developed massive mechanical hypersensitivity that started at 1 hr postinjection and reached its maximal effect between 6 and 24 hr postinflammation. Carrageenan-induced mechanical hypersensitivity returned to baseline levels at day 3 postinflammation in WT mice, whereas it persisted in GINIP$^{-/-}$ mice at this time point. Mechanical sensitivity of GINIP$^{-/-}$ mice returned to baseline levels only 7 days postinflammation (Figure 3B). In the chronic constriction injury (CCI) model using the 2 × 5 stimulations with increasing monofilaments method (Delfini et al., 2013; Descoeur et al., 2011), WT mice developed prototypical mechanical hypersensitivity during the first 2 weeks, which returned to baseline levels in the following 2 weeks. In GINIP$^{-/-}$ mice, CCI-induced mechanical hypersensitivity persisted during the 30 days trial, with all tested monofilaments (Figure 3C), suggesting that

GINIP is predominantly required for modulation of tissue injury-induced mechanical hypersensitivity.

Baclofen-Mediated Analgesia following Nerve Injury Is Impaired in GINIP$^{-/-}$ Mice

What are the mechanisms behind the prolonged injury-induced mechanical hypersensitivity observed in GINIP$^{-/-}$mice? Knowing that GINIP specifically interacts with $G_{\alpha i}$ proteins, we tested the ability of GINIP$^{-/-}$ mice to respond to the analgesic effect of three GPCR selective agonists: SNC-80 for the delta opioid receptor (DOR), DAMGO for the mu opioid receptor (MOR), and baclofen for metabotropic $GABA_B$ receptors ($GABA_B$-Rs). These agonists were tested under inflammatory and neuropathic pain. To model inflammatory pain, Carrageenan was injected in the hind paw of the mice, and to model neuropathic pain, we used the spared nerve injury model (Decosterd and Woolf, 2000) (Figure 4). At 1 day after Carrageenan injection, WT and GINIP$^{-/-}$ mice exhibited similar pronounced mechanical hypersensitivity (Figures 4A–4C). In agreement with a previous study (Smith et al., 1994), intrathecal injection (IT) of baclofen had no analgesic effect on either genotype (Figure 4A). However, administration of SNC80 strongly reversed Carrageenan-induced mechanical pain in both genotypes (Figure 4B), whereas DAMGO caused reduced, though significant, reversal of mechanical hypersensitivity both in WT and GINIP$^{-/-}$ mice (Figure 4C). In the SNI model, WT and GINIP$^{-/-}$ mice showed a profound and long-lasting mechanical hypersensitivity of the partially denervated hind paw (Figures 4D–4F). Importantly, IT injection of baclofen strongly reversed the mechanical hypersensitivity produced by nerve injury in WT mice but had no effect on GINIP$^{-/-}$ mice (Figure 4D). However, administration of SNC80 and DAMGO significantly decreased the mechanical hypersensitivity in both WT and GINIP$^{-/-}$ mice (Figures 4E and 4F), demonstrating that GINIP is selectively required for $GABA_B$-Rs-mediated, but not MOR- or DOR-mediated, analgesia in the neuropathic pain model used in this study.

Baclofen-Evoked Inhibition of HVA Ca^{2+} Channel Is Defective in GINIP-Deficient DRG Neurons

It is well described that most $G_{\alpha i/o}$-coupled GPCRs produce analgesia by controlling multiple downstream effectors, including inhibition of high-voltage-activated (HVA) Ca^{2+} channels to reduce neurotransmitter release from afferent and spinal neurons (Tatebayashi and Ogata, 1992), activation of inwardly rectifying K^+ channels to reduce excitability of pre- and postsynaptic spinal neurons (Takeda et al., 2004), and $G_{\alpha i/o}$-mediated inhibition of adenylyl cyclase to reduce cyclic AMP (cAMP) levels to counteract protein kinase A (PKA) activity (Tedford and Zamponi, 2006). Among these mechanisms, inhibition of presynaptic N-type HVA calcium channels has been described to play a prominent role in this process (Nockemann et al., 2013; Tedford and Zamponi, 2006). Thus, to address whether GINIP modulates GPCR signaling, we explored receptor-mediated inhibition of HVA Ca^{2+} channels in GINIP-expressing DRG neurons by taking advantage of the expression of the mcherry protein from *ginip* locus (Figure S2A). Using patch-clamp whole-cell recordings, we monitored the effects of SNC80-, DAMGO-, and baclofen-mediated inhibition of HVA Ca^{2+} channels on cultured heterozygous and homozygous mcherry$^+$ neurons. SNC80 and DAMGO had very little and similar effects on HVA Ca^{2+} channels of mcherry$^+$ neurons cultured from GINIP$^{+/-}$ and GINIP$^{-/-}$ mice (Figure 5A). In contrast, bath application of

baclofen induced strong inhibition of HVA Ca^{2+} channels in heterozygous neurons that was significantly reduced in GINIP$^{-/-}$ neurons (Figures 5A and 5B). The extent of baclofen-mediated inhibition of HVA Ca^{2+} channels in GINIP-expressing neurons is heterogeneous, suggesting differential expression of the $GABA_B$-Rs and/or Gβγ-sensitive HVA calcium channels in these neurons. Moreover, kinetics of baclofen inhibition washout showed a significantly faster time constant of current recovery in the absence of GINIP (1.68 ± 0.21 ms and 3.23 ± 0.19 ms for GINIP$^{-/-}$ and GINIP$^{+/-}$ respectively, n = 10–12, $p < 0.001$). These data demonstrate that baclofen-induced analgesia is impaired in GINIP$^{-/-}$ mice and suggest that $GABA_B$-Rs are highly enriched in GINIP^{+} neurons, whereas MOR and DOR are likely not expressed in these neurons. Indeed, double staining experiments show that MOR is virtually excluded from GINIP^{+} neurons (3.2% ± 0.82%) (Figure 5C) and DOR is expressed only in a very small subset of GINIP^{+} neurons (22.51% ± 2.94%) (Figure 5D), whereas virtually all GINIP^{+} neurons express $GABA_{B1}$ and $GABA_{B2}$ receptors (Figures 5E and 5F). Taken together, our electrophysiological and expression data reinforce and extend previous reports showing that baclofen has a greater effect on C fiber- than Aδ fiber-evoked glutamate release in the spinal cord (Ataka et al., 2000; Iyadomi et al., 2000) and that GINIP profoundly regulates $GABA_B$-induced intracellular signaling.

GINIP Also Modulates Adenylyl Cyclase Activity in Response to $G_{\alpha i}$-Coupled Receptors

To gain mechanistic insights into GINIP mode of action, we used an in vitro system in which we monitored the effect GINIP gain and loss of function on two distinct effectors: Cav2.2 channel and adenylyl cyclase in response to baclofen and DAMGO. To test the role of GINIP in modulation of $G_{\alpha i}$-protein regulation of Cav2.2 activity, human $Ca_v2.2$ channels were transiently expressed in tsA-201 cells along with rat β_{1b} and $\alpha_2\delta_{1b}$ auxiliary subunits, the human $GABA_{B1}$ and $GABA_{B1}$ receptors, or the rat MOR receptor. Whole-cell barium (Ba^{2+}) currents recordings showed that bath application of baclofen or DAMGO induced strong inhibition of Cav2.2 channel in the presence or absence of GINIP. In contrast, cells overexpressing GINIP displayed a significantly delayed time constant of current recovery from inhibition in response to both agonists (Figures 6A and 6B).

To unravel the role of GINIP in modulation of G protein regulation of adenylyl cyclase, we monitored intracellular cAMP level in tsA201 cells and in DRG neuronal cultures. In tsA201 cells, we used bioluminescence resonance energy transfer (BRET) (Barak et al., 2008). In this experiment, tsA-201 cells were transiently transfected with the EPAC biosensor, the human $GABA_{B1}$ and $GABA_{B2}$ receptors, or the rat MOR receptor in the presence or absence of GINIP. Following baseline measurement, cells were stimulated with 1 μM forskolin, either alone or together with 50 μM baclofen (Figures 6C and 6D) or 1 μM DAMGO (Figure S4). Forskolin stimulation induced a significant decrease in the BRET signal (red line), indicating an increase in cAMP levels. Forskolin-triggered decrease of BRET signal was significantly attenuated (blue line) in the presence of baclofen (Figures 6C and 6D) and DAMGO (Figure S4), indicating a decrease in cAMP levels. Importantly, baclofen- and DAMGO-mediated decrease of cAMP levels was strongly inhibited in cells overexpressing GINIP (Figures 6C, 6D, and S4), suggesting that GINIP uncouples $GABA_B$ and MOR from cAMP signaling. In control experiments, tsA-201 cells overexpressing GINIP alone (Figures 6C and 6D) or along with ProKR2, a Gαs-coupled receptor (Figure

S4), showed that GINIP does not modify the forskolin-mediated increase of cAMP, further demonstrating the selective association of GINIP with $G_{\alpha i}$ proteins.

To further address the role of GINIP in G protein regulation of adenylyl cyclase, we monitored intracellular cAMP levels directly in GINIP-expressing neurons using two-photon FRET imaging of the cAMP FRET sensor Epac-S^{H150} (Polito et al., 2013). Cultured heterozygous and homozygous $GINIP^{+}$ neurons were transduced with a recombinant Sindbis virus that allows rapid and highly efficient expression of Epac-S^{H150} (Gervasi et al., 2007; Hepp et al., 2007; Polito et al., 2013). In these conditions, mCherry fluorescence was too weak to be detected in $GINIP^{+}$ neurons. As GINIP is expressed in 95% of $IB4^{+}$ neurons, we used this isolectin to efficiently visualize GINIP-expressing neurons. Expression of Epac-S^{H150} was observed in 32% of $IB4^{+}$ neurons (52 cells out of 161). The effect of 50 μM baclofen on cAMP levels was evaluated by comparing the amplitude and the onset kinetics of two consecutive 1 min long bath applications of 5 μM forskolin, with baclofen being applied for 5 min prior to and during the second application of forskolin. In the absence of baclofen, two consecutive bath applications of forskolin produced similar increases of cAMP with similar amplitudes and onset kinetics in either genotype (data not shown). In the presence of baclofen, the mean amplitude of the second forskolin-evoked cAMP increase was similar to that measured in control conditions in the absence of baclofen (104% ± 4% and 97% ± 3% of control in $GINIP^{+/-}$ [n = 9] and $GINIP^{-/-}$ neurons [n = 8], respectively) (Figures 6E and 6F). In $GINIP^{+/-}$ neurons, baclofen did not affect onset kinetics of forskolin-induced response, as the ratio of slopes between the two-response onset was 1.03 ± 0.08 (n = 9). In contrast, the onset kinetics of the forskolin-mediated response was slower in the presence of baclofen in $GINIP^{-/-}$ neurons (slope ratio baclofen/control = 0.74 ± 0.06, $p < 0.05$, n = 8) (Figures 6E and 6G), indicating that loss of GINIP enhances baclofen-mediated inhibitory effect on adenylyl cyclase. These data are in agreement with the data obtained in tsA201 cells in which we show that overexpression of GINIP decreases DAMGO- and baclofen-mediated inhibitory effect on adenylyl cyclase. Together, our gain- and loss-of-function data demonstrate that GINIP plays a prominent role in modulation of $G_{\alpha i}$-coupled receptor signaling: it strongly interferes with the kinetics of inhibition of HVA Ca^{2+} channels and slightly affects the production of cAMP. Our data also demonstrate that GINIP can modulate $G_{\alpha i}$ signaling triggered by receptors other than $GABA_B$.

Baclofen-Mediated Presynaptic Inhibition Is Impaired in $GINIP^{-/-}$ Mice

To further characterize the mechanisms that cause the prolonged injury-induced mechanical hypersensitivity and impaired response to baclofen-induced analgesia in $GINIP^{-/-}$ mice, we measured synaptic transmission between primary afferent neurons and lamina II interneurons in the presence of baclofen (10 μM), SNC80 (20 μM), and DAMGO (1 μM). We performed whole-cell voltage clamp recordings in acute spinal cord slices while applying a pair of high-intensity electric stimulations on attached dorsal roots. We found that the average paired pulse ratio of evoked EPSCs (PPR) did not differ between WT (1.04 ± 0.102, n = 10; Figures 7A1 and 7A3) and $GINIP^{-/-}$ mice (0.912 ± 0.073, n = 18; Figures 7A2 and 7A3). However, following bath superfusion of baclofen (10 μM), the PPR was significantly increased in both WT (n = 10) and $GINIP^{-/-}$ (n = 18) mice (Figures 7A1–A3), indicating presynaptic inhibition of evoked response ($p < 0.001$). Interestingly, in these

conditions, the PPR was significantly higher in neurons recorded from WT mice (2.12 ± 0.034) than in neurons recorded from GINIP$^{-/-}$ mice (1.35 ± 0.162, $p < 0.05$), indicating an impaired baclofen-mediated presynaptic inhibition in GINIP$^{-/-}$ mice. In line with this observation, the average reduction in evoked EPSC amplitude was significantly more pronounced in neurons from WT (73.4% ± 3.5%) than from GINIP$^{-/-}$ mice (58% ± 4.5%, $p < 0.05$; Figure 7A4). In contrast, although the delta opioid agonist SNC80 (20 μM) induced a significant increase in PPR (Figures 7B1–7B3, $p < 0.05$), the average PPR following SNC80 superfusion did not differ in neurons from WT (2.01 ± 0.349, n = 10) and GINIP$^{-/-}$ (1.614 ± 0.204, n = 14) spinal slices. Similarly, the reduction in evoked EPSC amplitude caused by SNC80 superfusion was not significantly different between WT (52.7% ± 6.1%) and GINIP$^{-/-}$ (38.4% ± 7.8%) mice (Figure 7B4). Finally, the effect of mu opioid agonist DAMGO on PPR was very similar in WT (1.34 ± 0.15, n = 8) and GINIP$^{-/-}$ (1.73 ± 0.34, n = 11) spinal slices (Figure 7B3), and no difference was observed in the reduction of evoked EPSC amplitude between WT (38.1% ± 10.2%) and GINIP$^{-/-}$ (50.5% ± 7.2%) mice (Figure 7C4). Together, our data indicate that baclofen-induced presynaptic inhibition of synaptic transmission between primary afferent neurons and lamina II interneurons is impaired in GINIP$^{-/-}$ mice.

DISCUSSION

Peripheral nerve injury-evoked chronic pain induces complex changes in the GABAergic system, and primary sensory neurons have long been suggested to play a predominant role in this process. Indeed, electrophysiological recordings on spinal cord slices have shown that CCI and SNI models induce substantial reduction of primary afferent-evoked inhibitory postsynaptic currents (IPSCs) (Moore et al., 2002), and baclofen reduces the amplitude of primary afferent-evoked excitatory postsynaptic currents (EPSCs) (Ataka et al., 2000). Moreover, baclofen has a greater effect on C fiber- than Aδ fiber-evoked EPSCs, suggesting that the effect of baclofen is primarily due to $GABA_B$ receptors located at the terminals of C-unmyelinated nociceptors (Ataka et al., 2000). However, the molecular identities of the subpopulations of primary sensory neurons that are affected by this impairment of GABAergic inhibition are still unknown. In our study, we showed that GINIP is highly enriched in a subset of unmyelinated nonpeptidergic nociceptors that terminate within the outer and inner parts of the lamina II layer of dorsal horn spinal cord. Behavioral analyses showed that GINIP$^{-/-}$ mice exhibited a selective and prolonged tissue injury-induced mechanical hypersensitivity that was resistant to baclofen-mediated, but not MOR- or DOR-mediated, analgesia. GINIP-deficient DRG neurons displayed reduced inhibition of HVA Ca^{2+} channels and a slightly delayed forsolin-evoked production of cAMP in response to baclofen. Accordingly, baclofen-mediated presynaptic inhibition of lamina IIi spinal cord interneurons was severely impaired in GINIP$^{-/-}$ mice. These results provide compelling evidence supporting the role of primary sensory neurons, namely unmyelinated C fibers, in injury-induced modulation of spinal GABAergic inhibition and identify GINIP as a key modulator of peripherally evoked $GABA_B$-Rs signaling.

How could GINIP modulate $GABA_B$-Rs signaling? It is well established that agonist activation of $GABA_B$-Rs triggers conformational changes that cause heterotrimeric G proteins to dissociate into GTP-bound $G_{\alpha i}$ and $G\beta\gamma$. $G_{\alpha i}$-GTP inhibits adenylyl cyclase, and

Gβγ dimer inhibits Cav2 family of HVA Ca^{2+} channels (Tedford and Zamponi, 2006). The net output of $GABA_B$-R activation is a presynaptic inhibition of excitatory transmission in the spinal cord and reduced pain transmission. We showed that GINIP preferentially interacts with the active forms of $G_{\alpha i}$ proteins. Patch-clamp recordings of GINIP-expressing neurons showed that baclofen induced significant reduction of HVA Ca^{2+} channel activity in GINIP heterozygous neurons, and this reduction was significantly reduced in GINIP-deficient DRG neurons. Furthermore, overexpression of GINIP in tsA-201 cells strongly inhibited $G_{\alpha i}$-evoked decrease in cAMP levels and significantly increased the time constant of recovery from DAMGO- and baclofen-induced inhibition of Cav2.2 channels. Using cAMP-based FRET system, we showed that baclofen-mediated inhibition of cAMP production is slightly delayed, but not completely altered, in GINIP-deficient DRG neurons. Consistently, electrophysiological recordings of lamina IIi interneurons showed that baclofen-mediated presynaptic inhibition was severely impaired in $GINIP^{-/-}$ mice. In line with these in vitro data, our behavioral experiments showed that $GINIP^{-/-}$ mice were resistant to baclofen-mediated reversal of nerve injury-induced mechanical hypersensitivity, suggesting that GINIP/$G_{\alpha i}$-GTP interaction tightly regulates $G_{\alpha i}$-triggered modulation of HVA Ca^{2+} channels and adenylyl cyclase activities in vivo. How can $GINIP^{-/-}$ mice resistance to baclofen-mediated analgesia under neuropathic pain condition be explained? We favor the hypothesis that GINIP interferes with the kinetics of heterotrimeric G protein dissociation/association in response to baclofen. Loss of GINIP will favor rapid conversion of $G_{\alpha i}$-GTP to $G_{\alpha i}$-GDP form, causing rapid reassociation of $G_{\alpha i}$-GDP to Gβγ proteins, leading to rapid termination of baclofen-mediated G protein signaling. Rapid G protein signaling termination will cause a diminished inhibition of HVA Ca^{2+} channels and the maintenance of injury-induced high levels of cAMP. Diminished baclofen-induced inhibition of HVA Ca^{2+} channels in combination with the maintenance of high levels of cAMP will shift the balance toward increased excitability of afferent fibers and enhanced pain transmission. In line with this hypothesis, we showed that baclofen-mediated inhibition of HVA Ca^{2+} channels is strongly altered in GINIP-deficient DRG neurons and that these same neurons displayed a slight alteration of forskolin-mediated production of cAMP in response to baclofen. Whether HVA Ca^{2+} channels and adenylyl cyclase are the unique effectors of GINIP/$G_{\alpha i}$ interaction remains to be determined. Indeed, G protein-coupled inwardly rectifying K^+ channels, the major type of potassium channels, are important regulators of neuronal excitability, and their activation is tightly regulated by Gβγ proteins (Lüscher and Slesinger, 2010). A recent study has shown that GIRK channels are absent in mice primary sensory neurons, whereas these channels are functionally present in rat and human DRG neurons (Nockemann et al., 2013), suggesting that GINIP modulation of baclofen-mediated peripheral analgesia might be principally controlled by the extent of inhibition of HVA Ca^{2+} channels and adenylyl cyclase functions following $GABA_B$-R activation.

Our expression data also showed that GINIP is highly enriched in two molecularly and functionally distinct subpopulations of neurons: the cutaneous free nerve ending $MRGPRD^+$ neurons and C-LTMRs (Delfini et al., 2013; Li et al., 2011; Seal et al., 2009; Zylka et al., 2005). Recent studies have shown that the former population is involved in sensing acute and inflammation-induced mechanical stimuli (Cavanaugh et al., 2009; Shields et al., 2010) and the latter is specialized in sensing acute gentle touch and injury-induced mechanical and

chemical pain (Abrahamsen et al., 2008; Delfini et al., 2013; Li et al., 2011; McGlone et al., 2014; Seal et al., 2009; Zotterman, 1939). GINIP$^{-/-}$ mice had normal responses to thermal stimuli under acute and inflammatory conditions and exhibited a slightly perturbed response in the formalin test. In this test, GINIP$^{-/-}$ mice showed an early onset of formalin-evoked second pain response, reminiscent of that observed in mice lacking the type 4 metabotropic glutamate receptor (Vilar et al., 2013). The major phenotype observed in GINIP$^{-/-}$ mice consists of a selective and delayed mechanical hypersensitivity in the setting of neuropathic pain. This finding further supports the modality specificity view that argues that molecularly characterized subsets of primary sensory neurons are specialized in sensing and transducing well-defined sensory modalities (Abrahamsen et al., 2008; Cavanaugh et al., 2009; Delfini et al., 2013; Han et al., 2013; Seal et al., 2009; Shields et al., 2010; Vrontou et al., 2013). Indeed, we showed that IT injection of baclofen had no effect on Carrageenan-induced mechanical hypersensitivity in both WT and GINIP$^{-/-}$ mice. However, baclofen strongly reversed nerve injury-induced mechanical pain in WT, but not in GINIP$^{-/-}$ mice. Impaired reversal of nerve injury-induced mechanical pain in GINIP$^{-/-}$ mice was selective to baclofen, as SNC80 and DAMGO efficiently reversed SNI-induced mechanical hypersensitivity in these mice. Our expression data showed that MOR^{+} and GINIP^{+} neurons are mutually excluded from each other and that a significant number of GINIP^{+} neurons (22%) coexpress DOR. While GINIP/MOR mutual exclusion provides a straightforward explanation of DAMGO-mediated reversal of SNI-induced mechanical hypersensitivity in GINIP$^{-/-}$ mice, the strong SNC-80 effect in these mice is somehow puzzling. We hypothesize that SNC-80-mediated reversal of SNI-induced mechanical hypersensitivity in GINIP$^{-/-}$ mice mainly occurs through DOR activation in myelinated cutaneous A fibers (Bardoni et al., 2014; Scherrer et al., 2009). Indeed, it has been shown that ischemic block of myelinated axons abolishes touch-evoked neuropathic pain in human (Campbell et al., 1988). Furthermore, ablation of the vast majority of C fibers, including the specific ablation of MRGPPD^{+} neurons, does not alter nerve injury-induced mechanical hypersensitivity in mice (Abrahamsen et al., 2008; Cavanaugh et al., 2009). In line with this, our electrophysiological recordings showed that bath application of SNC-80 had no or very little effect on HVA Ca^{2+} channels in GINIP-expressing neurons, suggesting that DOR^{+}/GINIP^{+} small-diameter neurons play a minimal role in SNC-80-mediated analgesia in GINIP$^{-/-}$ mice.

Our in vitro studies revealed that GINIP can also modulate MOR-mediated inhibition of Cav2.2 channel and adenylyl cyclase in a similar manner to that of $GABA_B$-Rs, arguing that GINIP can be recruited upon activation of at least another $G_{\alpha i}$-coupled GPCR, thus opening avenues to deepen our understanding of GPCR biology. For instance, it is well established that regulators of G protein signaling (RGS proteins) play a key role in regulating GPCR activities. RGS proteins preferentially bind the active forms of Gα subunits and act as GTPase-activating proteins (GAPs) to accelerate (up to 1,000-fold) the rate of Gα-GTP hydrolysis, thereby limiting their lifetime under the active form (Hollinger and Hepler, 2002). Here we found that GINIP also preferentially binds to the GTP-bound forms of the three $G_{\alpha i}$ isoforms. We also showed that overexpression of GINIP inhibited DAMGO- and baclofen-induced decrease of cAMP levels and that loss of GINIP strongly reduced baclofen-induced inhibition of HVA Ca^{2+} channels. We hypothesize that GINIP and RGS

proteins might compete with each other to bind $G_{\alpha i}$-GTP proteins. GINIP binding to $G_{\alpha i}$-GTP will prevent RGS binding and blocks its GAP activity, causing a prolonged receptor-mediated activation. On the other hand, RGS binding to $G_{\alpha i}$-GTP will accelerate the rate of GTP hydrolysis and favors rapid reassociation of $G_{\alpha i}$-GDP with $G\beta\gamma$ subunits and termination of receptor-mediated activation. This hypothesis can provide a rational explanation of $GINIP^{-/-}$ mice resistance to baclofen-mediated analgesia, as $G_{\alpha i}$-GTP can only bind to RGS proteins that will accelerate its conversion to $G_{\alpha i}$-GDP, decreasing the length of receptor-mediated outcomes. Further dissection of the molecular mechanisms controlling the dynamics of GINIP and RGS proteins binding to the active forms of $G_{\alpha i}$ proteins will certainly deepen our understanding of G protein-coupled receptor signaling.

In conclusion, the results presented in this study are 3-fold: (1) they further consolidate the view of primary sensory neuron modality specificity, as we demonstrated that GINIP expression in a subset of nonpeptidergic nociceptors is required to selectively sense and transduce injury-induced mechanical pain; (2) they identify GINIP as a key modulator of primary sensory neurons-mediated regulation of the GABAergic system in the spinal cord; and (3) they identify GINIP as a modulator of $G_{\alpha i}$-coupled GPCRs. These findings indicate that targeting peripherally restricted $G_{\alpha i}$-coupled receptor agonists might maintain high levels of analgesic activity while significantly decreasing their well-established side effects. Further studies of the kinetics of GINIP modulation of $G_{\alpha i}$-triggered signaling pathway in response to $GABA_B$ receptor activation will deepen our understanding of the GABAergic inhibitory function in controlling pain transmission.

EXPERIMENTAL PROCEDURES

See Supplemental Experimental Procedures for further details.

Animals

All protocols are in agreement with European Union recommendations for animal experimentation. See Supplemental Experimental Procedures for a detailed description of the mice used.

In Situ Hybridization and Immunofluorescence

In situ hybridization and immunofluorescence were carried out following standard protocols (Moqrich et al., 2004). Briefly, animals were anesthetized and then transcardially perfused with 4% paraformaldehyde in phosphate-buffered saline (PBS). Then, DRGs and spinal cord were dissected, postfixed ON in the same fixative, and cryoprotected into a sucrose solution. Samples were sectioned at 12 μm (DRG section) or 16 μm (spinal cord section). Probes were hybridized overnight at 55°C, and the slides were incubated with the horseradish peroxidase anti-digoxigenin/fluorescein/biotin antibodies (Roche). Final detection was achieved using fluorescein/cy3/cy5 TSA plus kit (Perkin Elmer). For double fluorescent in situ experiments, the first antibody was inactivated using H_2O_2 treatment. For immunofluorescence, tissues sections were incubated in blocking solution for 1 hr at room temperature(RT), primary overnight at 4°C, and secondary antibody for 2 hr at RT. Acquisition of images was

performed on AxioImager Z1 (Zeiss). See Supplemental Experimental Procedures for further details.

Electrophysiology on Isolated DRG Neurons

Lumbar DRGswith attached rootswere dissected from adult GINIP heterozygote and null mice and were collected in Hank's balanced salt solution (HBSS) medium without calcium (Invitrogen). DRGs were prepared as in Delfini et al. (2013). Patch-clamp recordings were performed 12–28 hr after plating on mCherry-positive cellsvisualized with the epifluorescence connected tothe inverted Olympus IX70 microscope. For calcium current recordings, the extracellular solution contained (in mM): 2 $CaCl_2$, 100 TEACl, 2 NaCl, 1 $MgCl_2$, 40 choline Cl, 5 glucose, 5 4AP, 0.5 mg/ml BSA (pH 7.4 with TEAOH, ~330 mOsM). Pipettes with a resistance of 1–1.5 MΩ were filled with an internal solution containing (in mM): 110 CsCl, 3 $MgCl_2$, 10 EGTA, 10 HEPES, 3 Mg-ATP, 0.6 GTP (pH 7.4 with CsOH, ~300 mOsM). Drug application (DAMGO, SNC80, and baclofen) was performed as for recombinant channels in tsA201 cells.

Electrophysiology on Spinal Cord Slices with Attached Dorsal Root

Transverse spinal cord slices with attached dorsal roots from juvenile (P28–P44) $GINIP^{-/-}$ and WT mice were prepared for whole-cell recording as described in Delfini et al. (2013). Typically, a pair of high-duration (500 μs), high-intensity stimulations (350 μA) was used to recruit most primary afferent fibers in the recorded slice. A total of 20 consecutive paired stimulations with 5 s intervals were averaged. Paired pulse ratio was calculated as the ratio between the amplitude of the second and the first synaptic responses. Normalized synaptic responses were calculated by dividing the average response during drug application bytheaverage response measured in control.The protocol was repeated 5 times in control and 1,3,5, and 7 min after drug application (bath application for 1 min). The peak of the response (usually observed at 1 or 3 min) was used for statistical analysis. Liquid junction potentials (calculated value −16.5 mV) are not corrected for. SNC80 was purchased from Tocris, and DAMGO and baclofen were purchased from Sigma-Aldrich. SNC80 and DAMGO superfusion was achieved in the presence of 1 μM CGP55845A in orderto prevent an indirect action on paired pulse ratiothrough local GABAergic interneurons. Two-way ANOVA with repeated measures was used to compare the effects of drugs in WT and $GINIP^{-/-}$ mice. Student's t test, and signed-rank-sum test were used to compare the relative decrease in EPSC amplitude between different $GINIP^{+/+}$ and $GINIP^{-/-}$ mice.

Behavioral Assays

All behavioral analyses were conducted on littermate males 8–12 weeks old. Animalswere acclimated for 1 hrtotheirtesting environment priorto all experiments that were done at room temperature (~22°C). Student's t test was used for all statistical calculations. All error bars represent SEM. See Supplemental Experimental Procedures for a detailed description of all the behavioral tests used in this study.

Spared Nerve Injury Model of Neuropathic Pain—Spared nerve injury surgery was performed as described (Decosterd and Woolf, 2000). Briefly, mice were anesthetized with a mix of ketamine/xylazine while an incision was made through the skin and thigh muscle at

the level of the trifurcation of the sciatic nerve. The common tibial and peroneal nerve were ligated with 6.0 silk (Ethicon) and transected, leaving the sural nerve intact. Mechanical thresholds were determined 7 days after the surgery, before and after drug administration, and 30 days after the surgery. Mechanical threshold was determined using the up-down method.

Intrathecal Injections of Drugs—Animals were placed in habituation cages 1 hr prior to the administration of drugs. A total of 10 μl of each compound was injected intrathecally in unanesthetized mice. Successful placement of the needle was confirmed by flick of the tail. Baclofen (Sigma-Aldrich) was dissolved in H_20 solution (pH 7.6), SNC80 (Tocris Bioscience) was dissolved in 100 mM HCl solution, and DAMGO (Sigma-Aldrich) was dissolved in saline solution (0.9% NaCl). Response to mechanical stimulations was recorded 15 min after drug administration using the up-down method.

Supplementary Material

Refer to Web version on PubMed Central for supplementary material.

ACKNOWLEDGMENTS

We would like to thank Robert Kelly for his comments on the manuscript. We also thank members of the laboratory for scientific discussions, the IBDM imaging, and animal facilities for assistance. Thanks to the ARPEGE Pharmacology core facility at IGF and to Sebastien Leulier for his assistance with the BRET experiments. We are grateful to L.F. Reichardt for providing anti-TrkA antibody. G.S. is supported by NIH grant DA031777, and S.A.L. is supported by an HHMI Medical Research fellowship. This work has been funded by the ERC-starting grant, paineurons 260435. The authors declare that they have no competing financial interests.

REFERENCES

Abrahamsen B, Zhao J, Asante CO, Cendan CM, Marsh S, Martinez-Barbera JP, Nassar MA, Dickenson AH, and Wood JN (2008). The cell and molecular basis of mechanical, cold, and inflammatory pain. Science 321, 702–705. [PubMed: 18669863]

Agarwal N, Pacher P, Tegeder I, Amaya F, Constantin CE, Brenner GJ, Rubino T, Michalski CW, Marsicano G, Monory K, et al. (2007). Cannabinoids mediate analgesia largely via peripheral type 1 cannabinoid receptors in nociceptors. Nat. Neurosci 10, 870–879. [PubMed: 17558404]

Ataka T, Kumamoto E, Shimoji K, and Yoshimura M (2000). Baclofen inhibits more effectively C-afferent than Adelta-afferent glutamatergic transmission in substantia gelatinosa neurons of adult rat spinal cord slices. Pain 86, 273–282. [PubMed: 10812257]

Barak LS, Salahpour A, Zhang X, Masri B, Sotnikova TD, Ramsey AJ, Violin JD, Lefkowitz RJ, Caron MG, and Gainetdinov RR (2008). Pharmacological characterization of membrane-expressed human trace amine-associated receptor 1 (TAAR1) by a bioluminescence resonance energy transfer cAMP biosensor. Mol. Pharmacol 74, 585–594. [PubMed: 18524885]

Bardoni R, Tawfik VL, Wang D, François A, Solorzano C, Shuster SA, Choudhury P, Betelli C, Cassidy C, Smith K, et al. (2014). Delta opioid receptors presynaptically regulate cutaneous mechanosensory neuron input to the spinal cord dorsal horn. Neuron 81, 1312–1327. [PubMed: 24583022]

Campbell JN, Raja SN, Meyer RA, and Mackinnon SE (1988). Myelinated afferents signal the hyperalgesia associated with nerve injury. Pain 32, 89–94. [PubMed: 3340426]

Castro AR, Pinto M, Lima D, and Tavares I (2004). Nociceptive spinal neurons expressing NK1 and GABAB receptors are located in lamina I. Brain Res. 1003, 77–85. [PubMed: 15019566]

Cavanaugh DJ, Lee H, Lo L, Shields SD, Zylka MJ, Basbaum AI, and Anderson DJ (2009). Distinct subsets of unmyelinated primary sensory fibers mediate behavioral responses to noxious thermal and mechanical stimuli. Proc. Natl. Acad. Sci. USA 106, 9075–9080. [PubMed: 19451647]

Charles KJ, Evans ML, Robbins MJ, Calver AR, Leslie RA, and Pangalos MN (2001). Comparative immunohistochemical localisation of GABA(B1a), GABA(B1b) and GABA(B2) subunits in rat brain, spinal cord and dorsal root ganglion. Neuroscience 106, 447–467. [PubMed: 11591450]

Decosterd I, and Woolf CJ (2000). Spared nerve injury: an animal model of persistent peripheral neuropathic pain. Pain 87, 149–158. [PubMed: 10924808]

Delfini MC, Mantilleri A, Gaillard S, Hao J, Reynders A, Malapert P, Alonso S, François A, Barrere C, Seal R, et al. (2013). TAFA4, a chemokine-like protein, modulates injury-induced mechanical and chemical pain hypersensitivity in mice. Cell Rep 5, 378–388. [PubMed: 24139797]

Descoeur J, Pereira V, Pizzoccaro A, Francois A, Ling B, Maffre V, Couette B, Busserolles J, Courteix C, Noel J, et al. (2011). Oxaliplatin-induced cold hypersensitivity is due to remodelling of ion channel expression in nociceptors. EMBO Mol Med 3, 266–278. [PubMed: 21438154]

Dirig DM, and Yaksh TL (1995). Intrathecal baclofen and muscimol, but not midazolam, are antinociceptive using the rat-formalin model. J. Pharmacol. Exp. Ther 275, 219–227. [PubMed: 7562553]

Engle MP, Merrill MA, Marquez De Prado B, and Hammond DL (2012). Spinal nerve ligation decreases γ-aminobutyric acidB receptors on specific populations of immunohistochemically identified neurons in L5 dorsal root ganglion of the rat. J. Comp. Neurol 520, 1663–1677. [PubMed: 22120979]

Gangadharan V, Agarwal N, Brugger S, Tegeder I, Bettler B, Kuner R, and Kurejova M (2009). Conditional gene deletion reveals functional redundancy of GABAB receptors in peripheral nociceptors in vivo. Mol. Pain 5, 68. [PubMed: 19925671]

Gassmann M, Shaban H, Vigot R, Sansig G, Haller C, Barbieri S, Humeau Y, Schuler V, Muller M, Kinzel B, et al. (2004). Redistribution of GABAB(1) protein and atypical GABAB responses in GABAB(2)-deficient mice. J. Neurosci 24, 6086–6097. [PubMed: 15240800]

Gervasi N, Hepp R,Tricoire L, Zhang J, Lambolez B, Paupardin-Tritsch D, and Vincent P (2007). Dynamics of protein kinase A signaling at the membrane, in the cytosol, and in the nucleus of neurons in mouse brain slices. J. Neurosci 27, 2744–2750. [PubMed: 17360896]

Han L, Ma C, Liu Q, Weng HJ, Cui Y, Tang Z, Kim Y, Nie H, Qu L, Patel KN, et al. (2013). A subpopulation of nociceptors specifically linked to itch. Nat. Neurosci 16, 174–182. [PubMed: 23263443]

Hepp R, Tricoire L, Hu E, Gervasi N, Paupardin-Tritsch D, Lambolez B, and Vincent P (2007). Phosphodiesterase type 2 and the homeostasis of cyclic GMP in living thalamic neurons. J. Neurochem 102, 1875–1886. [PubMed: 17561940]

Hollinger S, and Hepler JR (2002). Cellular regulation of RGS proteins: modulators and integrators of G protein signaling. Pharmacol. Rev 54, 527–559. [PubMed: 12223533]

Hwang JH, and Yaksh TL (1997). The effect of spinal GABA receptor agonists on tactile allodynia in a surgically-induced neuropathic pain model in the rat. Pain 70, 15–22. [PubMed: 9106805]

Ibuki T, Hama AT, Wang XT, Pappas GD, and Sagen J (1997). Loss of GABA-immunoreactivity in the spinal dorsal horn of rats with peripheral nerve injury and promotion of recovery by adrenal medullary grafts. Neuroscience 76, 845–858. [PubMed: 9135056]

Iyadomi M, Iyadomi I, Kumamoto E, Tomokuni K, and Yoshimura M (2000). Presynaptic inhibition by baclofen of miniature EPSCs and IPSCs in substantia gelatinosa neurons of the adult rat spinal dorsal horn. Pain 85, 385–393. [PubMed: 10781911]

Janson W, and Stein C (2003). Peripheral opioid analgesia. Curr. Pharm. Biotechnol 4, 270–274. [PubMed: 14529429]

Jasmin L, Rabkin SD, Granato A, Boudah A, and Ohara PT (2003). Analgesia and hyperalgesia from GABA-mediated modulation of the cerebral cortex. Nature 424, 316–320. [PubMed: 12867983]

Laffray S, Bouali-Benazzouz R, Papon MA, Favereaux A, Jiang Y, Holm T, Spriet C, Desbarats P, Fossat P, Le Feuvre Y, et al. (2012). Impairment of GABAB receptor dimer by endogenous 14-3-3ζ in chronic pain conditions. EMBO J 31, 3239–3251. [PubMed: 22692127]

Latremoliere A, and Woolf CJ (2009). Central sensitization: a generator of pain hypersensitivity by central neural plasticity. J. Pain 10, 895–926. [PubMed: 19712899]

Legha W, Gaillard S, Gascon E, Malapert P, Hocine M, Alonso S, and Moqrich A (2010). stac1 and stac2 genes define discrete and distinct subsets of dorsal root ganglia neurons. Gene Expr. Patterns 10, 368–375. [PubMed: 20736085]

Li L, Rutlin M, Abraira VE, Cassidy C, Kus L, Gong S, Jankowski MP, Luo W, Heintz N, Koerber HR, et al. (2011). The functional organization of cutaneous low-threshold mechanosensory neurons. Cell 747, 1615–1627.

Lüscher C, and Slesinger PA (2010). Emerging roles for G protein-gated inwardly rectifying potassium (GIRK) channels in health and disease. Nat. Rev. Neurosci 77, 301–315.

McGlone F, Wessberg J, and Olausson H (2014). Discriminative and affective touch: sensing and feeling. Neuron 82, 737–755. [PubMed: 24853935]

Moore KA, Kohno T, Karchewski LA, Scholz J, Baba H, and Woolf CJ (2002). Partial peripheral nerve injury promotes a selective loss of GABAergic inhibition in the superficial dorsal horn of the spinal cord. J. Neurosci 22, 6724–6731. [PubMed: 12151551]

Moqrich A, Earley TJ, Watson J, Andahazy M, Backus C, Martin-Zanca D, Wright DE, Reichardt LF, and Patapoutian A (2004). Expressing TrkC from the TrkA locus causes a subset of dorsal root ganglia neurons to switch fate. Nat. Neurosci 7, 812–818. [PubMed: 15247919]

Nockemann D, Rouault M, Labuz D, Hublitz P, McKnelly K, Reis FC, Stein C, and Heppenstall PA (2013). The K(+) channel GIRK2 is both necessary and sufficient for peripheral opioid-mediated analgesia. EMBO Mol Med 5, 1263–1277. [PubMed: 23818182]

Patel S, Naeem S, Kesingland A, Froestl W, Capogna M, Urban L, and Fox A (2001). The effects of GABA(B) agonists and gabapentin on mechanical hyperalgesia in models of neuropathic and inflammatory pain in the rat. Pain 90, 217–226. [PubMed: 11207393]

Polito M, Klarenbeek J, Jalink K, Paupardin-Tritsch D, Vincent P, and Castro LR (2013). The NO/cGMP pathway inhibits transient cAMP signals through the activation of PDE2 in striatal neurons. Front Cell Neurosci 7, 211. [PubMed: 24302895]

Price GW, Kelly JS, and Bowery NG. (1987). The location of GABAB receptor binding sites in mammalian spinal cord. Synapse 7, 530–538.

Remondes M, and Schuman EM. (2003). Molecular mechanisms contributing to long-lasting synaptic plasticity at the temporoammonic-CA1 synapse. Learn. Mem 70, 247–252.

Scherrer G, Imamachi N, Cao YQ, Contet C, Mennicken F, O'Donnell D, Kieffer BL, and Basbaum AI (2009). Dissociation of the opioid receptor mechanisms that control mechanical and heat pain. Cell 737, 1148–1159.

Schuler V, Lüscher C, Blanchet C, Klix N, Sansig G, Klebs K, Schmutz M, Heid J, Gentry C, Urban L, et al. (2001). Epilepsy, hyperalgesia, impaired memory, and loss of pre- and postsynaptic GABA(B) responses in mice lacking GABA(B(1)). Neuron 37, 47–58.

Schwenk F, Baron U, and Rajewsky K (1995). A cre-transgenic mouse strain for the ubiquitous deletion of loxP-flanked gene segments including deletion in germ cells. Nucleic Acids Res. 23, 5080–5081. [PubMed: 8559668]

Seal RP, Wang X, Guan Y, Raja SN, Woodbury CJ, Basbaum AI, and Edwards RH (2009). Injury-induced mechanical hypersensitivity requires C-low threshold mechanoreceptors. Nature 462, 651–655. [PubMed: 19915548]

Shields SD, Cavanaugh DJ, Lee H, Anderson DJ, and Basbaum AI (2010). Pain behavior in the formalin test persists after ablation of the great majority of C-ffber nociceptors. Pain 757, 422–429.

Smith GD, Harrison SM, Birch PJ, Elliott PJ, Malcangio M, and Bowery NG (1994). Increased sensitivity to the antinociceptive activity of (-+/−)-baclofen in an animal model of chronic neuropathic, but not chronic inflammatory hyperalgesia. Neuropharmacology 33, 1103–1108. [PubMed: 7838323]

Takeda M, Tanimoto T, Ikeda M, Kadoi J, and Matsumoto S (2004). Activaton of GABAB receptor inhibits the excitability of rat small diameter trigeminal root ganglion neurons. Neuroscience 723, 491–505.

Tatebayashi H, and Ogata N (1992). Kinetic analysis of the GABAB-mediated inhibition of the high-threshold Ca2+ current in cultured rat sensory neurones. J. Physiol 447, 391–407. [PubMed: 1317434]

Tedford HW, and Zamponi GW (2006). Direct G protein modulation of Cav2 calcium channels. Pharmacol. Rev 58, 837–862. [PubMed: 17132857]

Towers S, Princivalle A, Billinton A, Edmunds M, Bettler B, Urban L, Castro-Lopes J, and Bowery NG (2000). GABAB receptor protein and mRNA distribution in rat spinal cord and dorsal root ganglia. Eur. J. Neurosci 72, 3201–3210.

Vilar B, Busserolles J, Ling B, Laffray S, Ulmann L, Malhaire F, Chapuy E, Aissouni Y, Etienne M, Bourinet E, et al. (2013). Alleviating pain hypersensitivity through activation of type 4 metabotropic glutamate receptor. J. Neurosci 33, 18951–18965. [PubMed: 24285900]

Vrontou S, Wong AM, Rau KK, Koerber HR, and Anderson DJ (2013). Genetic identification of C fibres that detect massage-like stroking of hairy skin in vivo. Nature 493, 669–673. [PubMed: 23364746]

Wang XL, Zhang HM, Chen SR, and Pan HL (2007). Altered synaptic input and GABAB receptor function in spinal superficial dorsal horn neurons in rats with diabetic neuropathy. J. Physiol 579, 849–861. [PubMed: 17218355]

Yang K, Wang D, and Li YQ (2001). Distribution and depression of the GABA(B) receptor in the spinal dorsal horn of adult rat. Brain Res. Bull. 55, 479–485. [PubMed: 11543948]

Zotterman Y (1939). Touch, pain and tickling: an electro-physiological investigation on cutaneous sensory nerves. J. Physiol 95, 1–28. [PubMed: 16995068]

Zylka MJ, Rice FL, and Anderson DJ (2005). Topographically distinct epidermal nociceptive circuits revealed by axonal tracers targeted to Mrgprd. Neuron 45, 17–25. [PubMed: 15629699]

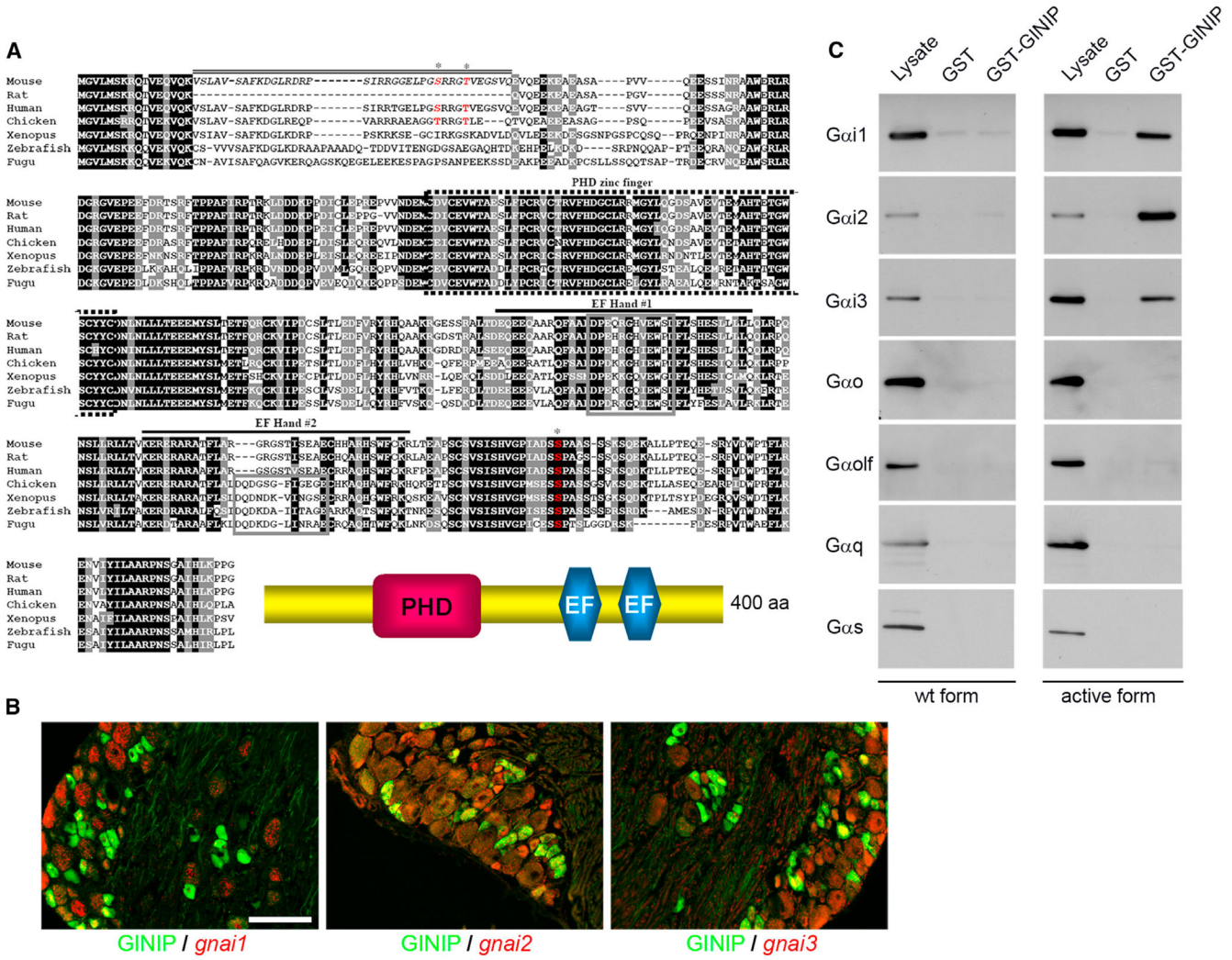

Figure 1. GINIP, a Highly Conserved Protein, Specifically Interacts with GTP-Bound Forms of $G_{\alpha i}$

(A) Alignment of amino acid sequences of GINIP from various vertebrate species. Residues shaded in black are identical in >85% of the predicted proteins; similar residues are highlighted in gray. The predicted PHD zinc finger (dotted box), the two EF-hand domains (#1 and #2; black lines), and the core domain of each EF-hand (gray box) are indicated. The sequence corresponding to the spliced exon in mouse is indicated by a double line. Phosphorylated residues identified by large-scale proteomic studies are indicated by asterisks (http://www.phosphosite.org/). Schematic representation of GINIP architecture is drawn on the bottom.

(B) In situ hybridization of DRGs with *gnai1*, *gnai2*, and *gnai3* antisense probes followed by immunostaining using rat anti-GINIP antibody. *gnai1* is mainly expressed in large neurons and excluded from $GINIP^+$ population, whereas *gnai2* and *gnai3* were mainly coexpressed with GINIP in smaller-diameter neurons. Scale bar, 100 μm.

(C) GST pull-down experiments: GST-GINIP (lanes 3 and 6) or GST alone (lanes 2 and 5) was incubated with lysate from HEK293 cells transfected with WT (lanes 1–3) or

constitutively active forms (lanes 4–6) of $G_{\alpha i}1$, $G_{\alpha i}2$, $G_{\alpha i}3$, Gαo, Gαolf, Gαq, and Gαs. All forms are fused with Venus protein. One-twentieth of the incubated volume of lysate was loaded in lanes 1 and 4. Western blot performed with anti-GFP antibody shows a specific interaction of GINIP with the active forms of only the three $G_{\alpha i}$ variants.

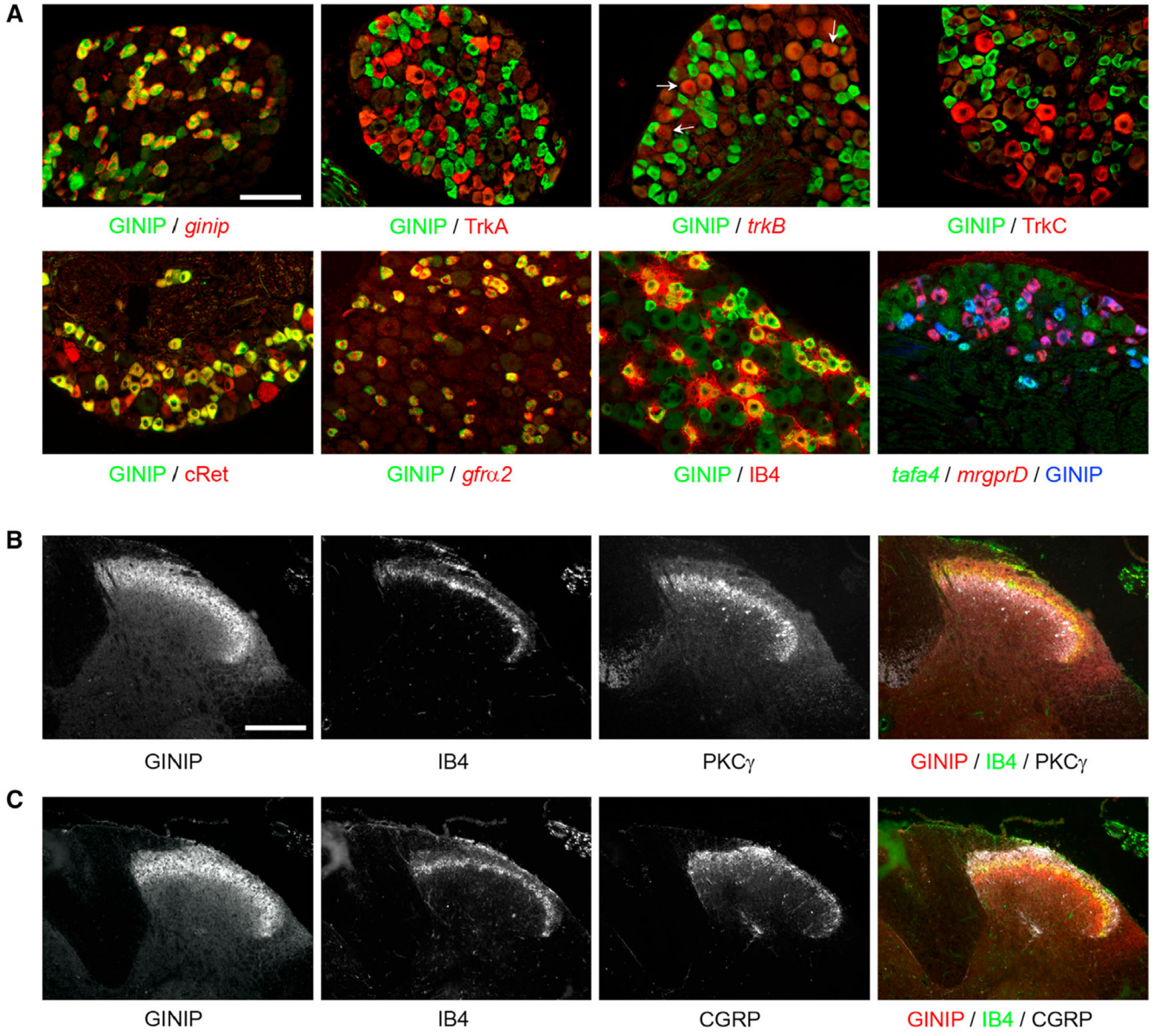

Figure 2. GINIP Defines a Subset of Nonpeptidergic Nociceptors that Targets Lamina II

(A) Characterization of GINIP-positive population in DRGs. Double immunostaining using rat anti-GINIP antibody associated with rabbit anti-TrkA or goat anti-cRet or goat anti-TrkC antibodies or Alexa 565-conjugated isolectin-B4. In situ hybridization using antisense probes for *ginip*, *trkB*, or *gfrα2* followed by immunostaining using rat anti-GINIP antibody. Double in situ hybridization using *mrgprD* and *tafa4* antisense probes followed by immunostaining using rat anti-GINIP antibody. The GINIP population can be divided into two subpopulations: *mrgprD*$^+$ and *tafa4*$^+$ neurons. Scale bar, 100 μm.

(B) Triple immunostaining using rat anti-GINIP and rabbit anti-PKCγ antibodies in combination with Alexa 488-conjugated isolectin-B4 on spinal cord sections.

(C) Triple immunostaining using rat anti-GINIP, rabbit anti-CGRP antibodies, and Alexa 488-conjugated isolectin-B4. Colabeled GINIP/IB4 fibers innervate lamina IIo. GINIP$^+$/

IB4^{-} fibers target lamina IIi PKCγ^{+} interneurons. Lamina I (CGRP staining) is devoid of GINIP staining. Scale bar, 100 μm. See also Figure S1.

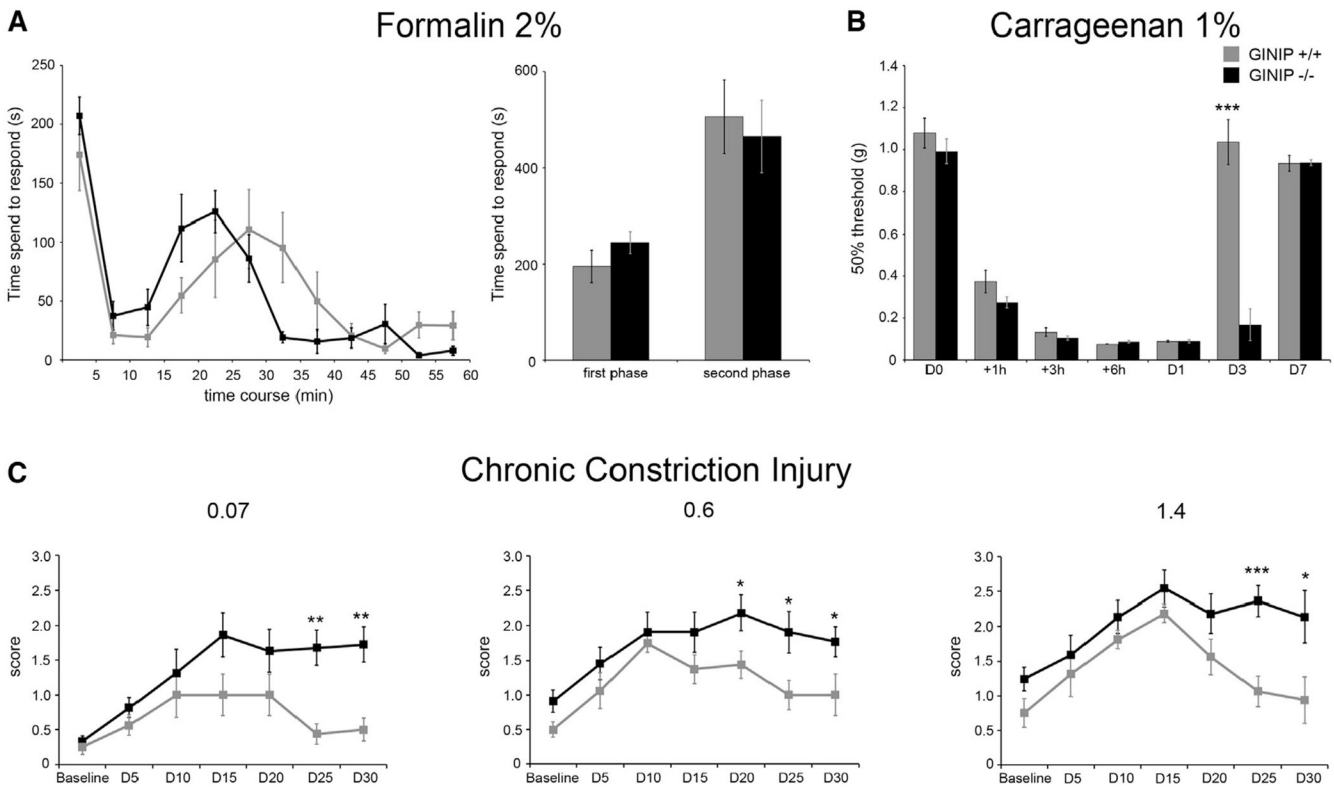

Figure 3. GINIP$^{-/-}$ Mice Exhibit Prolonged Mechanical Pain in Carrageenan and Chronic Constriction Mouse Model

(A) Nocifensive behavior of WT and GINIP$^{-/-}$ mice in response to 2% formalin injection in hind paw (n = 9 and n = 8, respectively). Both genotypes exhibited the same nociceptive duration during the first and second phase. Note that the second phase appears earlier in GINIP$^{-/-}$ compared to their WT littermates.

(B) Time course analysis of mechanical threshold of WT and GINIP$^{-/-}$ mice (n = 6 and n = 9, respectively) after 1% Carrageenan injection. GINIP$^{-/-}$ mice developed a prolonged mechanical pain in Carrageenan model compared to WT littermates (***p < 0.001).

(C) Time course presenting mechanical sensitivity following CCI of GINIP$^{-/-}$ mice (n = 11) and WT littermates (n = 8) using three different filaments of increasing calibers (0.07, 0.6, and 1.4 g). Baselines were determined before, and measures were performed every 5 days after CCI. WT and GINIP$^{-/-}$ mice developed characteristic mechanical hypersensitivity of CCI model. However, pain is prolonged in GINIP$^{-/-}$ mice and lasted during the whole 30-day trial. See also Figure S3.

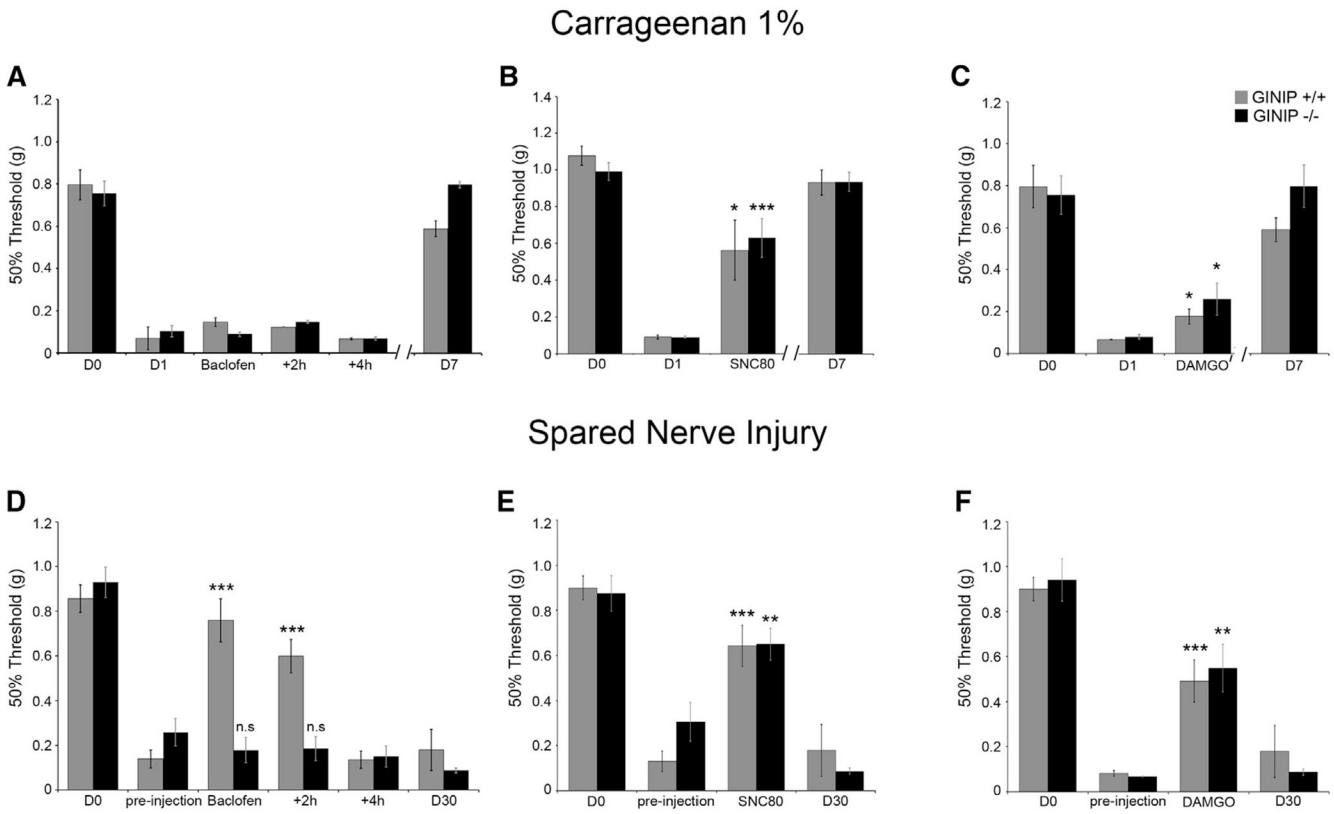

Figure 4. Baclofen-Mediated Analgesia following Nerve Injury Is Impaired in GINIP$^{-/-}$ Mice

(A–C) Mechanical responses of WT and GINIP$^{-/-}$ mice following 1% Carrageenan injection and IT injection of 0.1 μg of baclofen (A), 10 nmol of SNC80 (B), or 0.2 nmol of DAMGO (C). Injection of baclofen has no effect on mechanical hypersensitivity, whereas SNC80 or DAMGO reversed mechanical hypersensitivity in both genotypes (n = 6 for WT and n = 9 for GINIP$^{-/-}$) (*p < 0.05; ***p < 0.001).

(D–F) Mechanical responses of WT and GINIP$^{-/-}$ mice following SNI and IT injection of 0.1 μg of baclofen (D), 10 nmol of SNC80 (E), or 0.2 nmol of DAMGO (F). Injection of baclofen reversed mechanical hypersensitivity in WT mice, but not in GINIP$^{-/-}$ mice (n = 11 for both genotypes). Injection of SNC80 or DAMGO reversed mechanical hypersensitivity in both genotypes (n = 7 for GINIP$^{-/-}$ and n = 8 for WT) (**p < 0.01; ***p < 0.001).

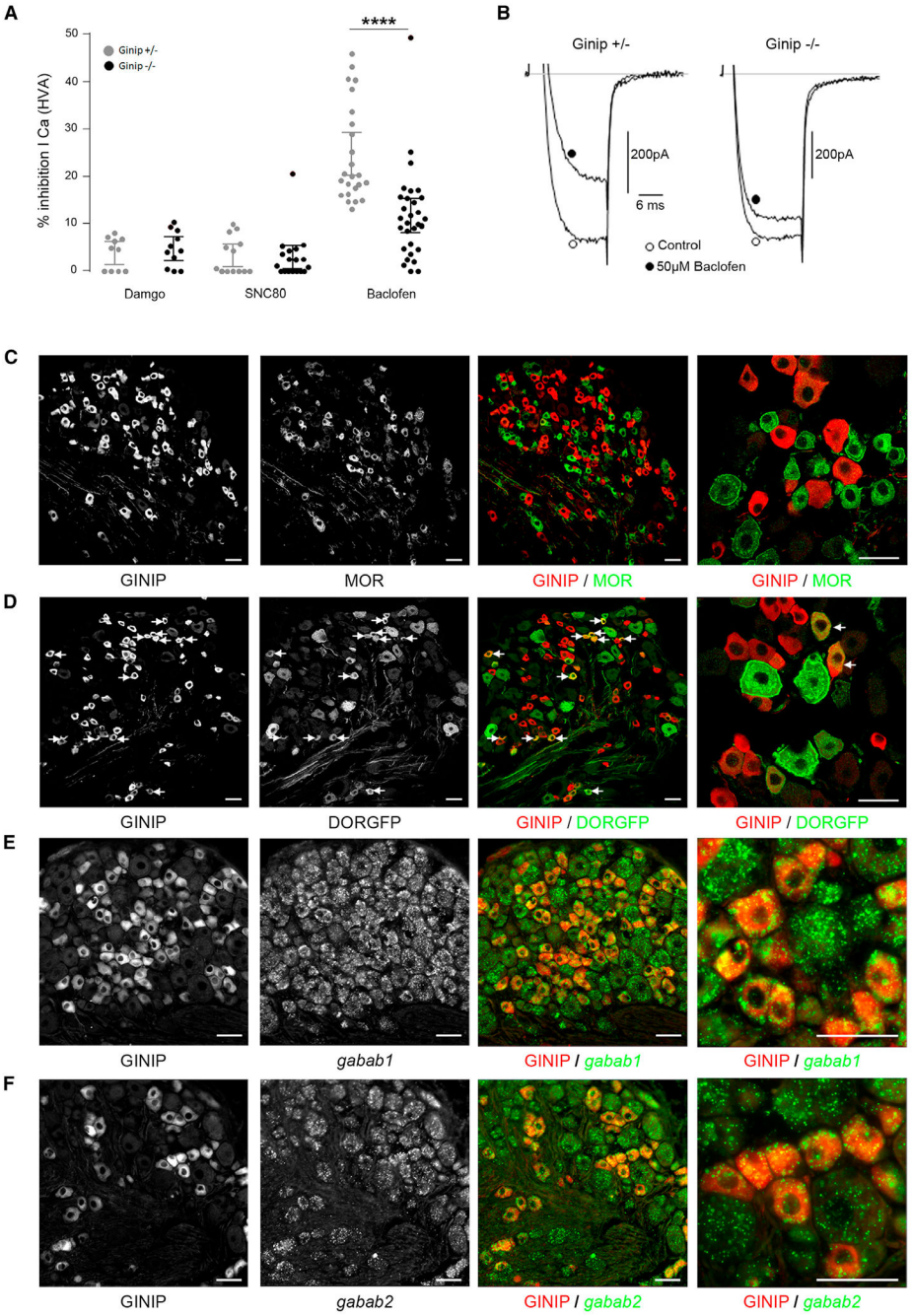

Figure 5. GINIP Is Selectively Expressed in GABA$_B$-Rs$^+$, but Not in MOR$^+$ or DOR$^+$ Neurons

(A) Summary of the maximal inhibition produced by SNC80 (1 μM), DAMGO (1 μM), and baclofen (50 μM) of high-voltage-activated calcium currents recorded from mCherry-positive DRG neurons from either GINIP$^{+/-}$ (gray circles) or GINIP$^{-/-}$ mice (black circles). Bars in the histogram represent the mean current inhibition ± SEM. Each circle represents an individual cell tested. HVA currents were elicited by 20 ms long test pulses to 10 mV from a holding potential of −80 mV.

(B) Typical traces of current inhibition produced by baclofen in mCherry-positive DRG neurons from the two genotypes.
(C and D) Double immunostaining using anti-MOR (C) or anti-GFP (D) in combination with rat anti-GINIP antibody.
(E and F) In situ hybridization using antisense probes for *gababr1* (E) and *gababr2* (F), followed by immunostaining using rat anti-GINIP antibody. Scale bars, 40 μm.

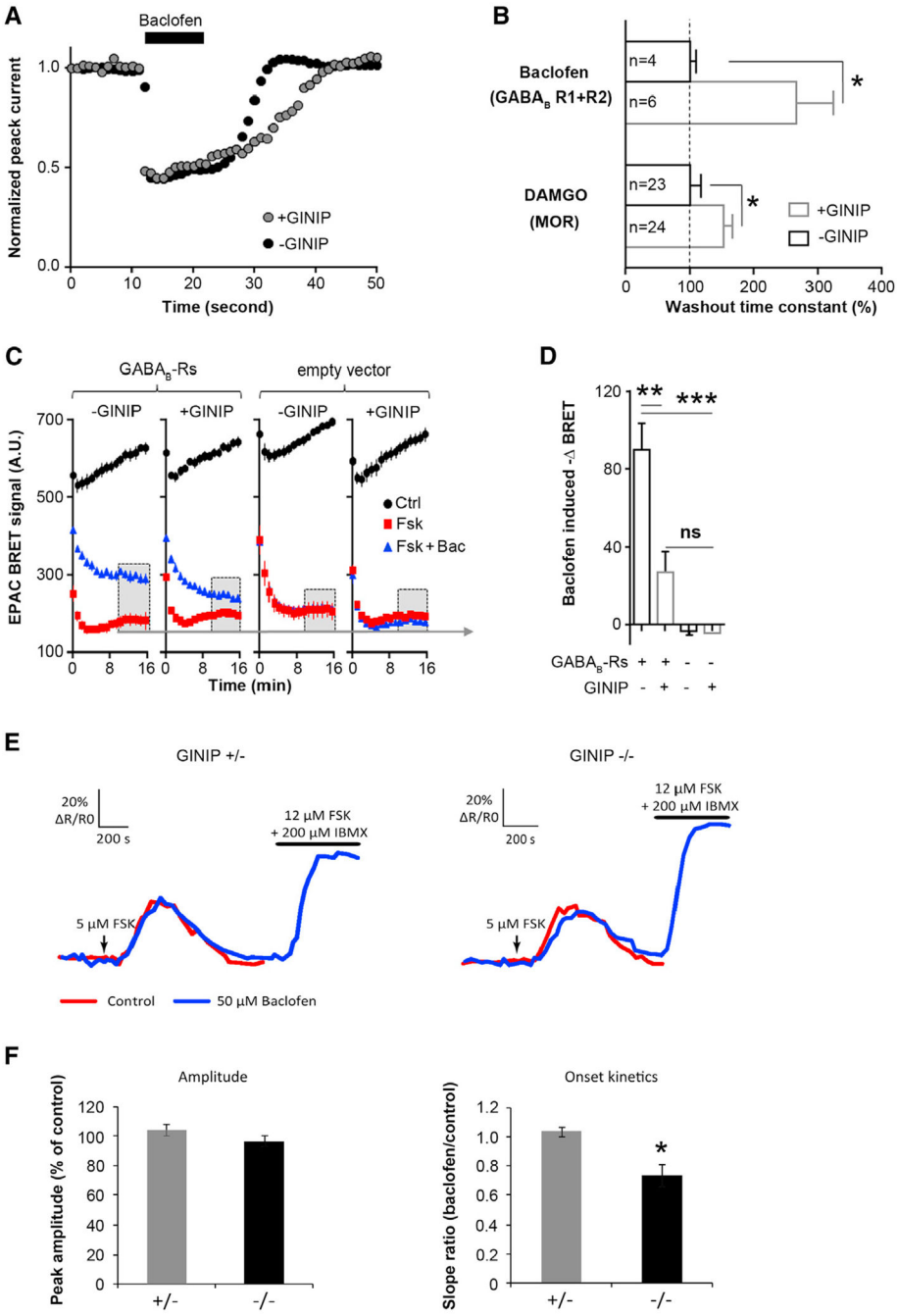

Figure 6. GINIP Modulates HVA Ca^{2+} Channels and cAMP Levels in Response to Baclofen

(A) Typical example of the time course of baclofen-induced N-type barium current inhibition in tsA201 cells expressing recombinant Cav2.2 channels and $GABA_B$ receptors in the presence (gray circles) or absence (black circles) of GINIP-GFP. Currents were evoked by a short 5 ms test pulse to +10 mv from −80 mv given at 1 Hz. Note the slow termination of baclofen inhibition in the presence of GINIP.

(B) Summary of the agonist washout kinetics for experiments similar to (A) for $GABA_B$ or MOR receptors coexpressed with Cav2.2. The washout time constant was normalized to the

value in the absence of GINIP (filled bars) compared to the values in the presence of GINIP (open bars).

(C) Baclofen-induced changes in the BRET ratio determined in tsA201 cells expressing $GABA_B$ receptors or an empty vector in the presence or absence of GINIP. The BRET ratio decreases during forskolin stimulation (red), and this decrease is significantly attenuated in the presence of baclofen (blue). Overexpression of GINIP inhibits baclofen-mediated reduction of FSK-triggered decrease in BRET ratio.

(D) Bar graph of the changes in BRET ratio determined in experiments as in (C).

(E) Traces show the increase in cAMP observed with Epac-S^{H150} in one $IB4^+$ neuron from GINIP heterozygous (left) and homozygous (right) cultures. The two consecutive responses to forskolin were overlaid for comparison. The 1 min application of 5 μM forskolin is indicated by an arrow. Combined application of forskolin and the phosphodiesterase inhibitor IBMX was used to control the sensor's saturation.

(F) A 5 min baclofen application prior to the second forskolin stimulation does not affect the amplitude of the second response (left) but decreases the onset kinetics of the response in GINIP-deficient DRG neurons as indicated by the significantly decreased slope ratio (right). Data are presented as the mean ± SEM and compared with a t test.

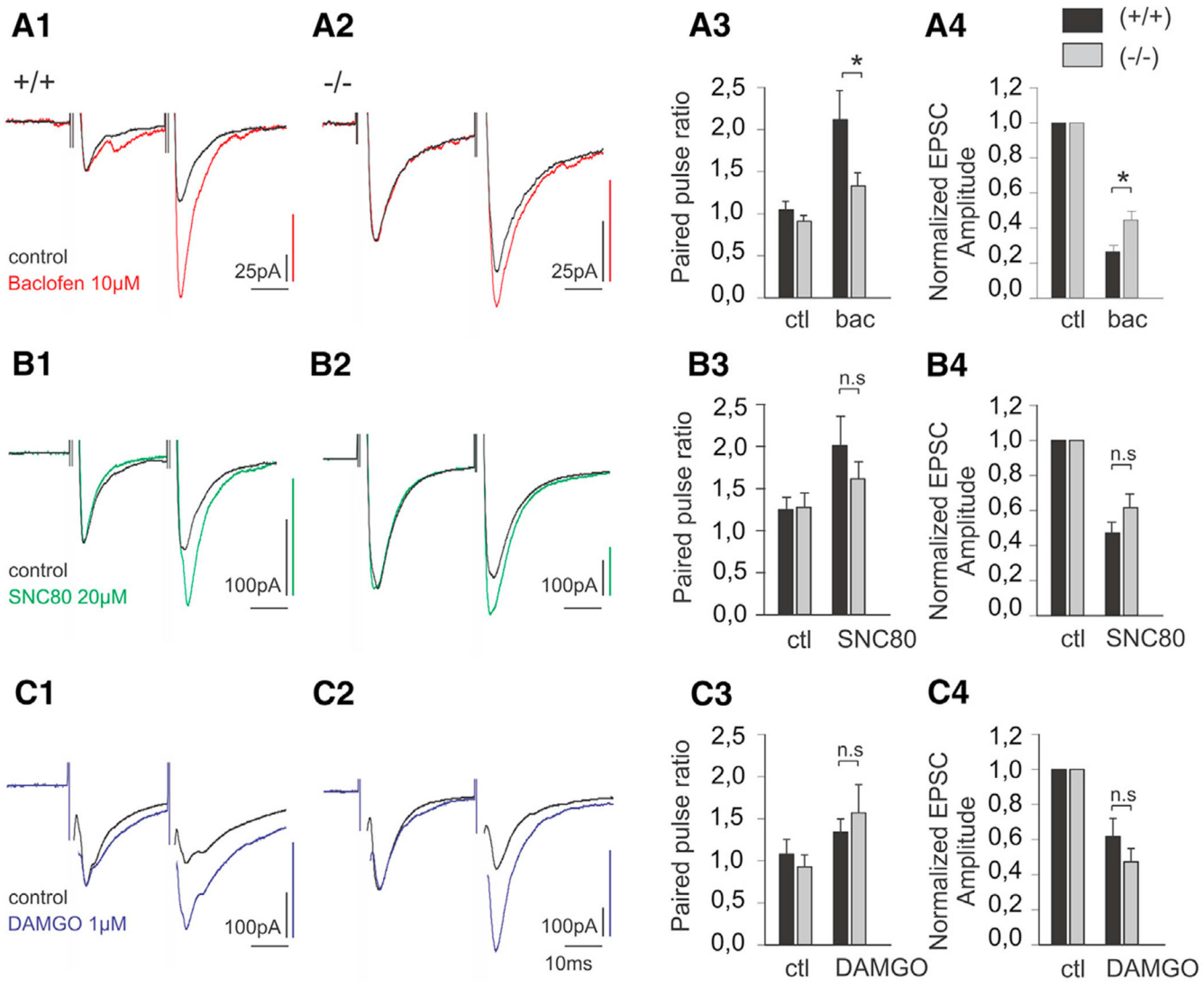

Figure 7. Modulation of Synaptic Transmission in GINIP Null Mice

(A) Normalized whole-cell voltage clamp recordings of EPSCs evoked by a pair of electric shock on attached dorsal root in WT (A1) and GINIP$^{-/-}$ (A2) animal lamina II neurons, in control and following superfusion of baclofen (10 μM). (A3) Paired pulse ratio of evoked EPSCs in control and following baclofen bath application in WT and GINIP$^{-/-}$ mice. (A4) Normalized evoked EPSC amplitude in control and following baclofen superfusion.

(B) Normalized whole-cell voltage clamp recordings of EPSCs evoked by a pair of electric shock on attached dorsal root in WT (B1) and GINIP$^{-/-}$ (B2) animal lamina II neurons, in control and following superfusion of SNC80 (20 μM). (B3) Paired pulse ratio of evoked EPSCs in control and following SNC80 bath application in WT and GINIP$^{-/-}$ mice. (B4) Normalized evoked EPSC amplitude in control and following SNC80 superfusion.

(C) Normalized whole-cell voltage clamprecordings of EPSCs evoked by a pair of electric shock on attached dorsal root in WT (C1) and GINIP$^{-/-}$ (C2) animal lamina II neurons, in control and following superfusion of DAMGO (1 μM). (C3) Paired pulse ratio of evoked

EPSCs in control and following DAMGO bath application in WT and GINIP$^{-/-}$ mice. (C4) Normalized evoked EPSC amplitude in control and following DAMGO superfusion. Traces in A1, A2, B1, B2, C1, and C2 have been scaled in order to facilitate the comparison of PPR (*$p < 0.05$).